Expert Systems With Applications 302 (2026) 130579

Contents lists available at ScienceDirect

Expert Systems With Applications

journal homepage: www.elsevier.com/locate/eswa

An ergonomic zone polyhedral representation-based mathematical program to prevent work-Related musculoskeletal risks

Marianna Ciccarelli [a,*], Michele Germani [a,b], Fabrizio Marinelli [c], Alessandra Papetti [a], Andrea Pizzuti [d]

[a] Department of Industrial Engineering and Mathematical Sciences (DIISM), Marche Polytechnic University, Via Brecce Bianche 12, 60131, Ancona, Italy
[b] IRCCS INRCA, Via Santa Margherita 5, 60124, Ancona, Italy
[c] Information Engineering Department (DII), Marche Polytechnic University, Via Brecce Bianche, 12, 60131, Ancona, Italy
[d] Department of Theoretical and Applied Sciences (DiSTA), E-Campus University, Via Isimbardi, 10, 22060, Novedrate, Italy

ARTICLE INFO

Keywords:
Manufacturing
Ergonomics
Work-related musculoskeletal disorders
Mathematical programming
Multi-objective optimization
Intelligent decision-support systems

ABSTRACT

The human-centric approach of Industry 5.0 underscores the integration of advanced technologies and information systems to enhance worker well-being, productivity, and safety. Significant progress has been made in automation and digitalization; however, the high prevalence of work-related musculoskeletal disorders (WRMSDs) remains a critical challenge, translating into a significant socioeconomic burden. Nevertheless, industrial practice still predominantly relies on observational ergonomic assessment methods and reactive ergonomic strategies, creating an urgent need for flexible, proactive, individualized, and easy-to-implement risk mitigation approaches. This paper addresses this gap by proposing an intelligent decision-support system based on a multi-objective optimization model that integrates heterogeneous information - workers' anthropometric measures, task requirements, and personal habits - within an expert-system architecture for industrial applications. The method relies on a convex integer program that can be embedded in machine controllers to compute the relative position between the product and the operator, minimizing ergonomic risks. Key innovations include the adoption of ergonomic principles without complex inverse kinematics, the explicit involvement of workers to account for their preferences, and the joint consideration of tasks involving both visual and physical interaction with the product. Experimental validation was conducted in a virtual environment simulating typical manufacturing scenarios, with diverse users and products. Results showed significant reductions in ergonomic risks with optimized positions, especially for smaller products, whereas larger ones posed challenges due to their size and task distribution. Statistical analyses validated these findings, highlighting the model's potential to reduce the REBA (Rapid Entire Body Assessment) risk index and enhance operational efficiency. Overall, the proposed system provides actionable set-points for workstation configuration and practical guidance for implementation, thus supporting human-centric manufacturing in Industry 5.0.

1. Introduction

The human-centric pillar of Industry 5.0 emphasizes the central role of humans in manufacturing processes, aiming to enhance well-being, safety, and skills development through the integration of advanced technologies and industrial information systems. The new paradigm encourages a harmonious and symbiotic relationship between humans and machines, in which automation supports workers by relieving them from repetitive and physically demanding tasks, enabling them to focus on higher-value activities (Longo et al., 2020). The aim is to reduce work-related health issues while improving productivity, efficiency, and job satisfaction (Lu et al., 2022). Within the human-centric framework of Industry 5.0, which integrates digital twins, collaborative robots, and emerging wireless technologies to enable mass personalization and human-machine collaboration, the prevention of WRMSD requires an adaptive, data-driven solution (Maddikunta et al., 2022).

Work-related musculoskeletal disorders (WRMSDs) are the most significant occupational health issue affecting workers in various industries and occupations (Korhan, 2019). WRMSDs affect muscles, tendons, ligaments, nerves, and other soft tissues, primarily in the neck, shoulders, upper and lower limbs. These disorders can result in pain, discomfort, and functional limitations and, in severe cases, lead to long-term

* Corresponding author.
E-mail addresses: m.ciccarelli@univpm.it (M. Ciccarelli), m.germani@univpm.it (M. Germani), fabrizio.marinelli@univpm.it (F. Marinelli), a.papetti@univpm.it (A. Papetti), andrea.pizzuti@uniecampus.it (A. Pizzuti).

https://doi.org/10.1016/j.eswa.2025.130579
Received 22 September 2025; Received in revised form 15 November 2025; Accepted 23 November 2025
Available online 4 December 2025

disability. According to the Bureau of Labor Statistics, WRMSDs accounted for 29 % of all non-fatal occupational injuries in the US in 2020, while the European Agency for Safety and Health at Work (EU-OSHA) reports that they represent approximately half of all occupational diseases in Europe (De Kok et al., 2019). The economic impact of WRMSDs is also substantial, with costs related to medical treatment, rehabilitation, lost productivity, absenteeism, and early retirement estimated in billions of euros each year.

Certain sectors are particularly prone to WRMSDs, such as healthcare, agriculture, construction, manufacturing, transport, and logistics, where workers are exposed to repetitive movements, forceful exertions, working in awkward or uncomfortable positions, vibrations, and inadequate ergonomic design of workstations, tools, and equipment. The relevance of the problem has led to the diffusion of many ergonomic assessment techniques that consider these risk factors (Joshi & Deshpande, 2019). The causes of WRMSDs are often multifactorial, and addressing them requires a comprehensive approach that includes ergonomic design, training, and awareness programs, as well as risk assessment. Worker involvement, consultation, and participation in decision-making processes are encouraged to create a safe and healthy work environment.

Industry 5.0 technologies offer new opportunities to support this shift (Pistolesi et al., 2024). Collaborative robots can assist in physically demanding tasks, such as heavy lifting, and provide ergonomic support, avoiding excessive force exertion. The implementation of ergonomic design principles in the development of machinery, equipment, and workstations (e.g., adjustable heights, proper body positioning, and user-friendly interfaces) can contribute to improved worker posture and reduced strain on the musculoskeletal system. Wearable technologies enable posture monitoring and feedback, alerting workers when they assume poor postures or perform movements that increase the risk of WRMSDs. In parallel, data analytics can identify high-risk patterns in task execution, allowing for proactive implementation of preventive measures. Crucially, the successful integration of these technologies depends not only on their technical deployment but also on workers' ability and willingness to adopt new habits and ergonomic practices.

However, implementing ergonomic interventions is still a challenge. Numerous barriers impede the effective execution of initiatives aimed at preventing musculoskeletal disorders (MSDs), including limited time, resources, communication challenges, and a lack of knowledge (Yazdani & Wells, 2018). Early detection and intervention play a crucial role in preventing the progression of WRMSDs. However, health-compromising behaviors are difficult to change (Schwarzer, 2008). Increased awareness and knowledge can help individuals make informed decisions and take proactive measures to protect their musculoskeletal health. Yet, changes in organizational settings are often unsuccessful due to the non-consideration of the psychological domain (Winum et al., 1997). Few ergonomic training programs address this aspect (Mohammadi Zeidi et al., 2011). Changing habits takes time and persistence, so consistency, reinforcement, and ongoing support are key to successfully addressing this challenge.

This work addresses these challenges by proposing an optimization model that adapts the product position to the workers' anthropometric measures, product characteristics, task requirements, and workers' habits. The module implements an individualized, preventive ergonomic strategy and acts as a behavioral nudge: by delivering workstation setpoints that naturally afford healthy postures, it supports gradual habit change without requiring explicit posture reconstruction. It engages workers in the process of identifying and solving ergonomic challenges, encouraging them to provide feedback on their experiences, criticalities, and suggestions for improvement. These aspects are inputs to the model.

The rest of the paper is organized as follows. Section 2 critically analyzes key scientific literature on occupational safety and health management, focusing on the evolution from reactive to proactive strategies and the role of simulation, digital human models (DHM), and optimization techniques in mitigating ergonomic risks. Section 3 presents the proposed multi-objective optimization model, which integrates risk polyhedra projections and obstacle constraints to optimize worker positioning. Section 4 outlines the experimental validation of the model and presents its main findings. Section 5 discusses the results, emphasizing strengths, limitations, and suggestions for future research directions.

2. Literature review

Occupational safety and health management typically relies on a short-term reactive approach, despite the imperative to transition towards a more preventive, or ideally proactive, strategy (Nord Nilsson & Vänje, 2018). Instead of merely assessing risks of activities and implementing corrective measures, it is crucial to intervene during the design phase to proactively mitigate potential risks. In this context, simulation and DHM play a crucial role in replicating task and worker dynamics (Dammacco et al., 2022). By integrating ergonomic considerations, one can assess various scenarios of product placement and determine the most ergonomic arrangement. Facility layout optimization models also strive to minimize ergonomic risks by accounting for factors like reach distances, work postures, and movement patterns (Mårdberg et al., 2018). These models leverage mathematical programming, simulation, or heuristic algorithms to optimize the configuration of workstations, equipment, and products within a workspace while mitigating musculoskeletal risk. For instance, Otto and Scholl (2011) incorporated ergonomic assessments into a mixed-integer programming model for assembly line balancing, demonstrating significant reductions in OCRA scores. More recently, Zhang et al. (2024) addressed assembly line balancing with mixed products and multi-manned stations by explicitly modeling human factors-such as worker skills and assignments-and proposed a model with a multi-objective solution approach to balance energy consumption and cost, reporting improvements over recent methods. Complementarily, Eswaran et al. (2024) studied layout planning for human-robot collaborative assembly and validated the resulting configurations through immersive extended reality tools, showing how model-driven configuration can support system-level decisions prior to deployment.

This strategic integration of operational research and ergonomics has also been emphasized in recent reviews addressing fatigue and musculoskeletal risks (Xu & Hall, 2021). Wang et al. (2023) proposed an anthropometric data-driven evaluation method, incorporating two artificial intelligence algorithms in tandem to design intricate console layouts.

The creation of ergonomic workplaces necessitates a concurrent focus on dynamic and adaptive work design, factoring in both human and productivity-related information. The survey by Otto and Battaïa (2017) illustrates that optimization models for assembly line balancing and job rotation scheduling, which integrate ergonomic risk estimation methods, outperform conventional task-to-station and worker-to-station assignments. Bautista et al. (2016) proposed an innovative approach to solve the assembly line balancing problem by simultaneously considering temporal, spatial, and ergonomic attributes. Similarly, Nourmohammadi et al. (2023) introduced a mixed-integer linear programming model that addresses three key objectives: cycle time, maximum ergonomic risk of workstations, and total ergonomic risks. Rahman et al. (2023) examined semi-automatic assembly lines by explicitly modeling human factors (operator age and skill) and jointly optimizing cycle time, energy consumption, and ergonomic risk under uncertain processing times. In the disassembly domain, Wu et al. (2023) studied two-sided line balancing with explicit human-robot interaction, proposing a model and a dedicated search method that jointly balance the number of stations, line smoothness, robot energy consumption, and disassembly cost.

Limited research has focused on optimizing working conditions with a specific aim to improve posture. This emphasis on posture optimization is more prevalent in the domain of product design. For example, Liu et al. (2020) presented a product ergonomic optimization approach

based on a posture load regulatory network and quality function deployment theory. To virtually assess the impact of design choices on product usability while reducing costs and time, Nakajima et al. (2022) employed an evolutionary optimization technique minimizing hand-muscle effort.

Enabling real-time and dynamic actions during operators' work necessitates the automation of human pose recognition, which generally involves the use of vision-based systems for reconstructing a person's skeleton and calculating joint angles. Subsequently, considerable efforts are dedicated to addressing the challenge of posture prediction or reconstruction, employing both machine learning and optimization techniques. Ma et al. (2009) presented a multiple-objective optimization (MOO) which considers fatigue and joint discomfort, for posture analysis and prediction, albeit limited to static scenarios. Advancing posture prediction, Marler et al. (2009) introduced a MOO that combines human performance measures, including joint displacement, musculoskeletal discomfort, and a variation on potential energy. Gragg et al. (2013) proposed an optimization-based method aimed at determining an accurate and efficient solution to the posture reconstruction problem, minimizing the distance between joint centers in the simulation model and those in the corresponding experimental subjects. Recent research by Gomes et al. (2022) proposed a multi-objective optimization framework to generate human motions that simultaneously minimize multiple ergonomic indicators, effectively addressing conflicts that arise when optimizing single ergonomic scores. However, their model was developed and validated exclusively on a digital human mannequin in simulation environments, without considering the practical implementation of the optimized trajectories in actual work scenarios.

The adoption of sensor-free posture monitoring systems in real work contexts is still hindered by various barriers, such as the complexity of posture reconstruction and prediction models, hardware settings, the occlusion problem, privacy implications, and more (Rodrigues et al., 2022; Zhang et al., 2020). Exploring simpler alternative solutions through intelligent human-machine collaboration could be a promising avenue for investigation. An example of automatic and adaptive solution preventing MSDs is to position the products to be processed according to appropriate criteria. However, there is limited specific research on optimization models specifically focused on product placement to reduce WRMSDs. Ongoing research focuses on human-robot collaboration (HRC) using human kinematic models (Busch et al., 2017), enabling robots to adapt physical assistance based on human fatigue or position objects for worker convenience. A representative contribution in this direction is provided by El Makrini et al. (2022), who proposed a virtual element-based postural optimization method in HRC scenarios. Their approach enables collaborative robots to dynamically reposition the workpiece based on real-time posture optimization and effectively reducing ergonomic risks. However, these approaches often require further refinement to align with current international safety regulations or to be effectively implemented in real industrial settings. Beyond HRC, Nguyen et al. (2016) presented a system that adjusts the workpiece pose using a height-adjustable platform to facilitate task completion in a natural working posture. Similarly, Merikh-Nejadasl et al. (2021) introduced an algorithm monitoring worker joint positions and orientations to recommend the most ergonomic posture for task completion, employing Rapid Entire Body Assessment (REBA) and Forward and Backward Reaching Inverse Kinematic (FABRIK) methods to assess optimized posture feasibility. Dalle Mura and Dini (2019) suggested a software tool based on a genetic algorithm to enhance the adaptability of the assembly process to individual worker characteristics, notably considering the physical energetic limits of workers when assigning tasks to workstations.

As revealed by the comparison shown in Table 1, the literature is divided into two main areas of research. The first focuses on optimizing line balancing, with the goal of distributing or minimizing ergonomic risk exposure, but without directly optimizing posture. The second area, often linked to HRC, aims at optimizing postures or trajectories in real-time, almost universally relying on inverse kinematics methods and invasive tracking systems (vision-based or sensor-based), which consequently hinder industrial implementation. This proposal distinguishes itself from both. Unlike balancing methods, it targets a preventive optimization by acting on the work setting (product-operator positioning) rather than just assignment. Furthermore, although studies exist that consider operator skills and physical characteristics, the model presented here explicitly incorporates the operator's preferences into the operational constraints. By offering a sensor-free solution that integrates fundamental ergonomic principles directly into convex integer programming, the approach overcomes the computational and hardware limitations imposed by inverse kinematics and tracking.

In particular, this work contributes to the field by proposing a convex integer programming-based decision-support module that can be integrated into a machine controller for ergonomic settings. Grounded on ergonomic principles, the model computes the product-operator positioning that minimizes associated risks. Key innovations include:

- Avoiding posture prediction and reconstruction problem. The model incorporates ergonomic principles, such as the golden and strike zones, directly into constraints, eliminating the need for inverse kinematics.
- Tailored solutions designed for individual workers. The program uses customized parameters that address each worker's specific needs and habits, directly involving workers in defining constraints and encouraging their commitment to adopting ergonomic practices.
- Behavioral change techniques. Applying techniques to facilitate behavioral change helps workers break old habits and develop new ones naturally, integrating posture improvement into their workflow (i.e., the product position defined by the mathematical program should imply that the operator adopts an ergonomic posture accordingly).
- Suitable for a mass customization and mass personalization paradigm. The mathematical program considers product and task characteristics to generate the working conditions, including both visual and physical interaction with the product.

By integrating these aspects, the proposed mathematical program strives to advance the state of the art in ergonomic optimization, promoting safer and more adaptive workplaces.

3. Material and methods

This section presents the convex integer program that constitutes the core of the intelligent decision-support approach. The model operationalizes ergonomic principles and translates worker- and task-specific data into actionable workstation configurations. First, the decision problem is formalized and the ergonomic principles incorporated into the model are described. Then, the core concept of risk polyhedra is introduced, followed by the formulation of the complete multi-objective optimization model.

3.1. Problem description

The production process consists of a set T of tasks that must be carried out sequentially on the product by an operator. Although each task could, in principle, require a different product position, we assume that the product remains fixed[1] within a feasible region $S \subseteq R^3$, with its bottom-left-front corner located, without loss of generality, at coordinates $(0, 0, 0)$. The region S is defined according to workplace features, product sizes, and technological constraints, such as the reachable points of the handling machine that holds the product at the gripping point.

[1] Fixing the product position is a realistic assumption, as any repositioning would typically involve machine movements that introduce idle times and necessitate operator relocation to maintain safety conditions.

Table 1
Summary of reviewed studies.

Reference	Problem definition	Methodology	Physical ergonomic factors	Inverse kinematics	Tracking system
(Bautista et al., 2016)	Assembly line balancing problem with temporal, spatial, and ergonomic risk attributes.	MOO models.	Ergonomic risk (in ergo-seconds) based on standard assessment methods.	No	No
(Busch et al., 2017)	Postural optimization in HRC with acceptability, task constraints, and safety.	Gradient descent algorithm.	REBA score, acceptability (proxemics, laterality, visibility).	Yes	Yes
(Dalle Mura & Dini, 2019)	Assembly line balancing problem with ergonomics and workers' characteristics.	Genetic algorithm.	Oxygen consumption in performing micro movements.	No	No
(El Makrini et al., 2022)	Postural optimization in HRC with workpiece position.	Ordinary differential equations.	REBA score.	Yes	Yes
(Eswaran et al., 2024)	Layout planning problem for HRC assembly systems with task allocation and material handling.	Modified particle swarm algorithm.	Ergonomic factor (five levels) assigned to resources.	No	No
(Gomes et al., 2022)	Trajectory optimization for ergonomics enhancement in worker activities.	Non-dominated sorting genetic algorithm II.	RULA score, back flexion, normalized whole-body effort (torques at every joint).	Yes	Yes
(Gragg et al., 2013)	Optimization-based posture reconstruction for DHM.	Local-optimum solution methods.	Posture.	Yes	Yes
(Ma et al., 2009)	Posture prediction and analysis method with physical fatigue in manual operations.	MOO algorithm.	Physical fatigue, joint discomfort, joint torque capacity.	Yes	Yes
(Marler et al., 2009)	Posture prediction in DHM.	MOO algorithm.	Joint displacement, delta-potential-energy, discomfort (moving close to joint limits/ranges).	Yes	No
(Merikh-Nejadasl et al., 2021)	Optimal ergonomic posture for task completion in industry.	FABRIK method.	REBA score.	Yes	Yes
(Nguyen et al., 2016)	Working posture controller for adaptation of the work piece pose.	Optimization model and support vector machine.	EAWS score.	Yes	Yes
(Nourmohammadi et al., 2023)	Assembly line balancing problem with temporal and ergonomic risk attributes.	Enhanced non-dominated sorting genetic algorithm.	REBA score by IPS IMMA software.	No	No
(Otto & Scholl, 2011)	Assembly line balancing problem with nonlinear ergonomic risks.	SALOME and simulated annealing	Ergonomic risks (three levels) based on OCRA index.	No	No
(Rahman et al., 2023)	Assembly line balancing problem with temporal, energy consumption and ergonomic risks attributes.	Memetic algorithm with Q-learning and Monte-Carlo.	Ergonomic risk based on lifting risk, twisted wrist, twisting heap, and squat risk.	No	No
(Wang et al., 2023)	Complex console layout design with real-time anthropometric evaluation.	Multi-stage artificial neural network and genetic algorithm.	Posture, operational accessibility and visibility.	No	Yes
(Wu et al., 2023)	Two-sided disassembly line balancind problem with HRC, energy, and costs attributes.	Discrete squirrel search algorithm.	None.	No	No
(Zhang et al., 2024)	Assembly line balancing problem with multi-skilled workers.	Multi-objective co-evolutionary algorithm.	None.	No	No

Each task $t \in T$ is characterized by an estimated duration d^t and comprises a set I^t of one or several concurrent operations. Each operation $\tau \in I^t$ of task t affects one or more parts of the product and is therefore associated with a parallelepiped-shaped region, referred to as the *tolerance region* of τ. This region is defined by the coordinates $(s_x^\tau, s_y^\tau, s_z^\tau)$ of its origin, i.e., its bottom-left-front corner, and by its sizes $\epsilon_x^\tau, \epsilon_y^\tau$ and ϵ_z^τ (see Fig. 1).

The operator is allowed to move only within the S_{xy} plane[2] and is required to remain in a fixed position throughout the execution of all potentially concurrent operations of a task. Given the operator's *feet center*

[2] The z-coordinate is fixed at the floor level $\bar{w}_z$ since extensions or lowering movements are forbidden in order to maintain the desired ergonomic level.

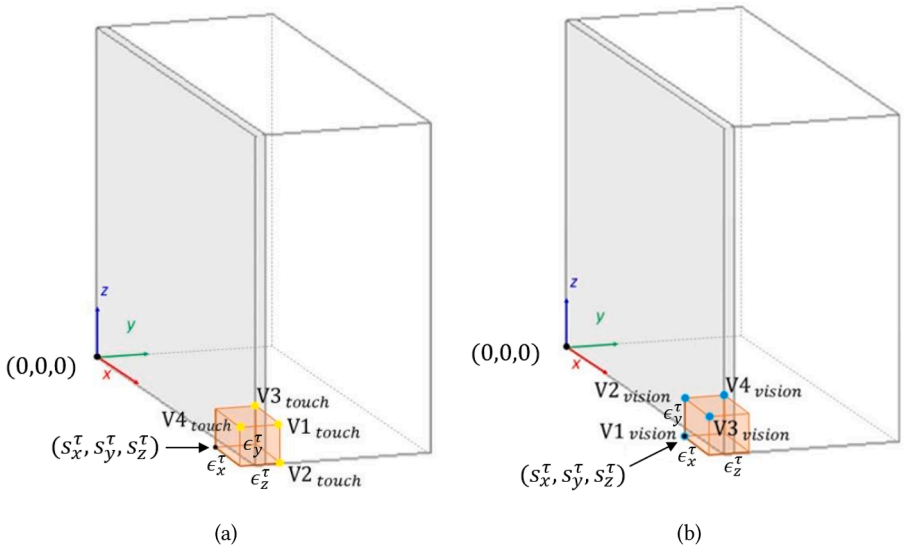

Fig. 1. Example of tolerance regions (in orange) of sizes $\epsilon_x^\tau, \epsilon_y^\tau$ and ϵ_z^τ for touch (a) and vision (b) tasks.

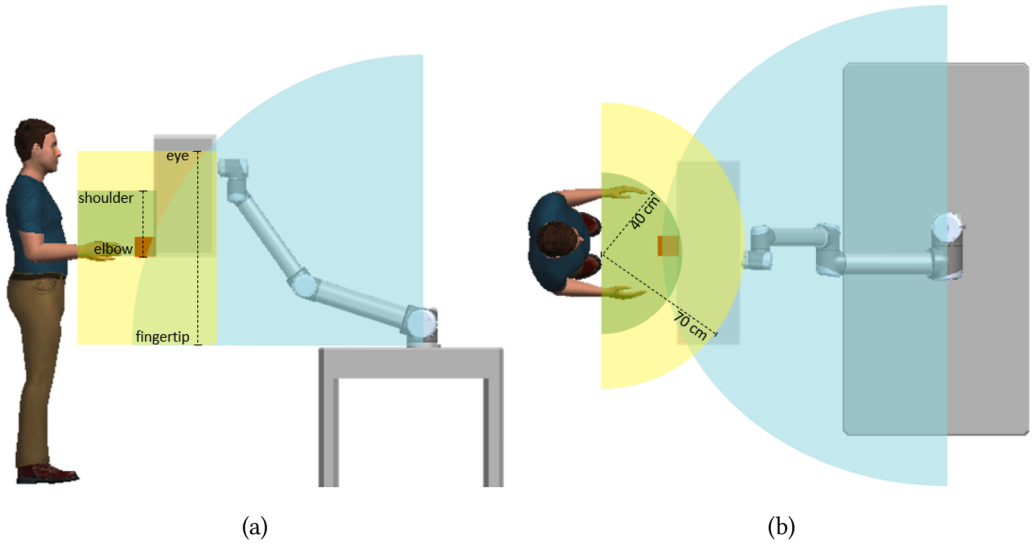

Fig. 2. Task's tolerance region in red. Golden and Strike zones in yellow and green. Reachable volume of the handling machine in light blue. (a) Strike zone; (b) Golden zone.

$(w_x^t, w_y^t, \bar{w}_z) \in S$, which represents the worker's position while performing task t, the ergonomic risk cost of task t can be inferred by considering the risk level where the tolerance regions of its operations fall, see Section 3.1.1. The Minimum-Risk Product-Operator Positioning problem can thus be formally stated as follows:

Problem 3.1. *Given a feasible region $S \subseteq R^3$, determine the operator feet centers $\mathbf{w}^t = (w_x^t, w_y^t, w_z^t) \in S$ for a sequence of tasks $t \in T$, such that the total ergonomic risk cost is minimized, and, in subsequent order, the total operator displacement (with respect to its habitual positions), and the total traveled distance are also minimized.*

3.1.1. Risk levels

An operation can either be of *touch* type, i.e., a manual activity, or *vision* type, i.e., an inspection activity. The set I^t of the operations of a given task t, however, must consist of operations of the same type. Therefore we refer to tasks as either *touch tasks* or *vision tasks*. .

For operations requiring direct contact between the operator's hands and the product, i.e., when the operation is of touch type, their risk level is determined by the tolerance region and the so-called *Golden* and *Strike zones*, Ciccarelli et al. (2022). The zones are modeled as concentric semi-cylinders in front of the operator, centered on his/her feet, whose radius depends on the level of active risk: 40 cm for risk-free level (green area), or 70 cm for low-risk level (yellow area), see Fig. 2. In particular, the Golden and Strike zones respectively identify the semi-cylinder projection on the S_{xy} and S_{yz} planes. The heights along the z axis of the Strike zone are determined according with the operator's anthropometric characteristics: risk-free area ranges from the elbow height up to the shoulder height, whereas low-risk area starts from the thigh quota up to the eye quota.

On the other hand, the vision operations are all linked to the operator's *Field of View*, which is modeled as a pseudo-cone 70 cm high, centered at the operator's eye level, and described by three angles α_1, α_2 and α_3. The pseudo-cone forms an isosceles triangle when projected onto the S_{xy}, and an irregular triangle when projected onto the S_{yz} plane, see Fig. 3. The vertex-angle of the isosceles triangle is α_1, whereas the angle at the eye operator of the irregular triangle is divided by the triangle height into below and above angles α_2 and α_3. Angles α_1, α_2 and α_3 are

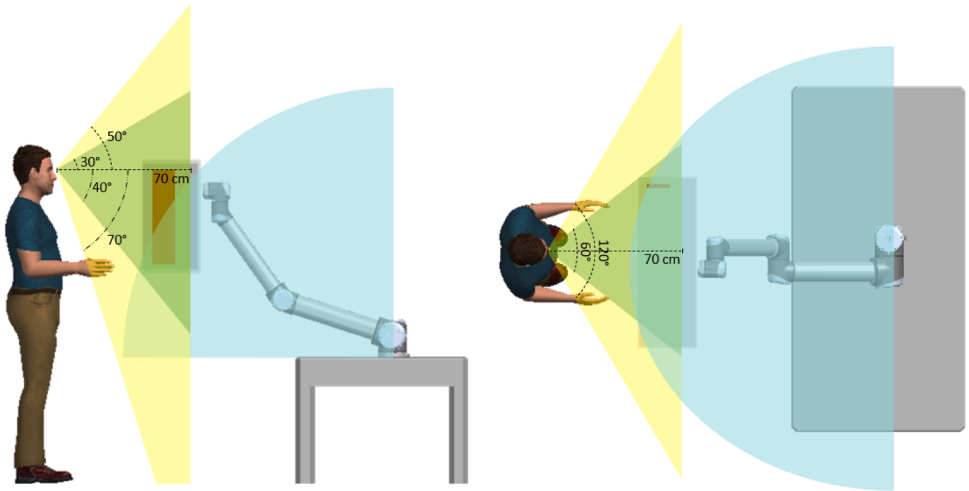

(a) (b)

Fig. 3. Task's tolerance region in red. Low-risk and risk-free zones in yellow and green, respectively. Reachable volume of the handling machine in light blue. (a) horizontal view; (b) vertical view.

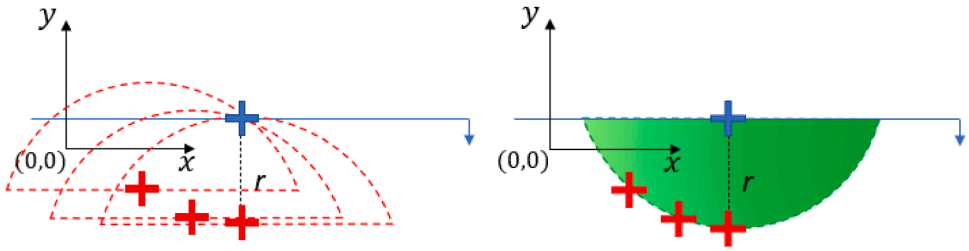

(a) (b)

Fig. 4. Blue cross is the origin (s_x^τ, s_y^τ) of an arbitrary tolerance region; (a) red crosses mark operator positions spanning the risk areas (dotted); (b) resulting risk-free zone for the operator (green area).

chosen to respect fixed boundaries within which the level of accuracy and resolution of the human eye meet the high standards required for visual inspections, and also depend on the level of active risk. For risk-free level (green area), $\alpha_1 = 60°$, $\alpha_2 = 40°$ and $\alpha_3 = 30°$, whereas for low-risk level (yellow area), $\alpha_1 = 120°$, $\alpha_2 = 70°$ and $\alpha_3 = 50°$. For both low- and free-risk levels, further angular spans are provided by limited neck rotations: 20° for α_1 and 10° for α_2, whereas no upward rotation is counted due to the relevant ergonomic risk.

Risk areas always guarantee a minimum distance: a *vital* distance ensuring enough space between the operator's body and the product during touch tasks, and a *sight focus* distance from the operator's eyes during vision tasks. Both distances are set to 5 cm.

To assign a risk level to the operation τ, it is enough to consider only the four reference vertices depicted in Fig. 1a and Fig. 1b for touch and vision operations, respectively. Indeed, it is easy to see that if V_1, V_2, V_3, and V_4, considered under the touch or vision cases, fall within the same risk area, then all the remaining vertices of the tolerance region do as well. The operation τ achieves the risk-free ergonomics level only if, for a given product position, all the reference vertices of its tolerance region are contained in the green area. On the other hand, τ is flagged at high ergonomic risk if at least one of the reference vertices violates the boundaries of the yellow area. A task t is at risk-free ergonomics level if all the operations in I^t is at risk-free level. Finally, ergonomic costs associated with risks are quantified by parameters $c_{free} < c_{low} \ll c_{high}$.

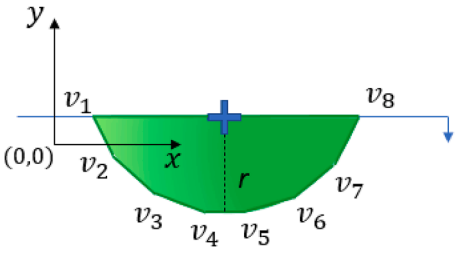

Fig. 5. the S_{xy} projection of the risk polyhedron generated by the set of points $V = \{v_1, \ldots, v_8\}$.

3.2. Risk polyhedra

Recall that the product is placed at a reference point $(0, 0, 0)$, hence the level of active risk of the operation τ depends solely on the relative positions between the reference points $(s_x^\tau, s_y^\tau, s_z^\tau)$ of its tolerance region, and the operator's feet center (w_x, w_y, w_z). The product reference point assumes that the gripping point and handling machine placement derive coherently from the product size, taking into account limitations on product repositioning due to inefficiency/safety. The deviation from the worker's habitual positions can be easily determined since the positions in historical settings can be translated to points in the reference system.

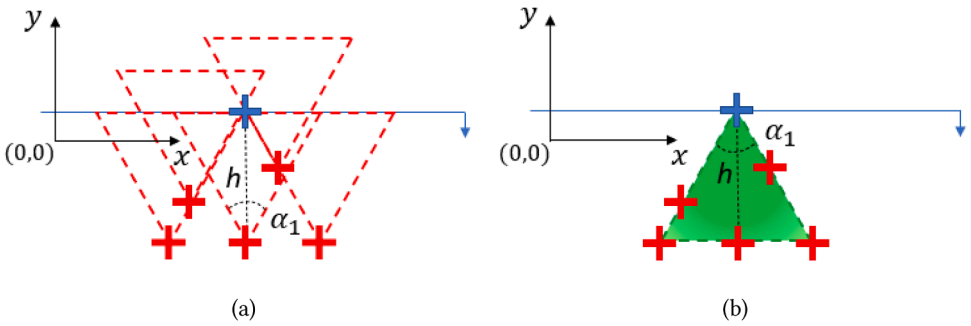

Fig. 6. Blue cross is the origin (s_x^τ, s_y^τ) of an arbitrary tolerance region; (a) red crosses mark operator positions spanning the risk areas (dotted); (b) resulting risk-free zone for the operator (green area).

Let us describe now the geometric objects upon which the proposed optimization model is based. For the Golden & Strike zones associated with a touch operation τ, the risk-free level (green area) is represented by a semi-cylinder centered on the operator feet center, whose projection onto the S_{xy} plane, i.e., the Strike zone, corresponds to a semicircle with a radius $r = 40$ cm. On this plane, only the operator position needs to be determined, being the product origin at $(0, 0)$, and the origin of the tolerance region of operation τ at (s_x^τ, s_y^τ). It is easy to see that all the positions in which the operator may accomplish the operation at risk-free level define a semicircle having the same radius r and centered at (s_x^τ, s_y^τ) (see Fig. 4).

Our aim is to incorporate into a convex integer programming model the check for an operator's position being in the risk area R. This area is a convex body which therefore corresponds to the convex hull of a given (possibly infinite) set of points V:

$$R = \left\{ \sum_{k=1}^{|V|} \lambda_k v_k \middle| \sum_{k=1}^{|V|} \lambda_k = 1, \lambda_k \geq 0 \ \forall k = 1, \dots, |V| \right\}. \tag{1}$$

In other words, R corresponds to all and only the convex combinations of points in V. To achieve this representation with a finite number of points, the semicircle R is approximated, by means of standard discretization techniques, to a polyhedron $\tilde{R}$, that we call *risk polyhedron* (see Fig. 5). Clearly, the approximation quality depends on the number of vertices used in the discretization.

The risk polyhedron $\tilde{R}$ of the Strike zone can be directly extended along the z coordinates ranging between elbow and shoulder heights, resulting in an approximated semi-cylinder.

The risk region associated with the Field of View zone of a vision task is derived similarly. As aforementioned, the pseudo-cone of the risk-free level defines an isosceles triangle of height $h = 70$ cm when projected on the S_{xy} plane, and all the positions in which the operator may accomplish the operation at risk-free level is a congruent triangle with vertex-angle at (s_x^τ, s_y^τ), see Fig. 6. The extension along the z axis is obtained by considering the angles α_2 and α_3 of the Field of View zones on the S_{yz} plane, which generates a pseudo-cone. The resulting risk polyhedron $\tilde{R}$ is derived by discretizing the base of the pseudo-cone into a two-dimensional polyhedron with vertices in V, and then connecting these vertices to the vertex-angle.

Finally, analogous results are obtained when referring to higher ergonomic levels of risk.

By representing active risk levels via the Golden & Strike or Field of View zones and discretizing them into risk polyhedra, we obtain an approximate yet convenient description of ergonomic risk levels. Indeed, this approach captures core elements needed for ergonomic risk estimation by abstracting away overly complicated real-world dynamics to foster computational efficiency.

3.3. Multi-objective optimization model

Recall that each task $t \in T$ possibly consists of a set I^t of concurrent operations, each with its own tolerance area, bottom-left-front corner in $(s_x^\tau, s_y^\tau, s_z^\tau)$ and sizes $(\epsilon_x^\tau, \epsilon_y^\tau, \epsilon_z^\tau)$. Recall, moreover, that an operation τ can be performed at a risk-free level of ergonomics only if all the reference vertices of its tolerance region are contained in the green area. Since in the new reference system we are computing the operator's feet center, the previous condition corresponds to checking whether the feet center is contained within all the risk polyhedra associated with the reference vertices of the tolerance region of τ. To address this point and for the sake of convenience, from now on, each operation τ in I^t is replaced by four operations with point-sized tolerance zones and origins at the four reference vertices of the tolerance region of τ. We then refer to the origin of the tolerance zone of operation τ as the origin of τ.

Let $Q = \{free, low\}$ be the set of risk levels for operation/task fulfillment (*high* risk is kept separated and used at convenience). For each $q \in Q$, let $V_q^{\tau t}$ be the set of vertices $\mathbf{v}_{1q}^{\tau t}, \dots, \mathbf{v}_{mq}^{\tau t}$ of the risk polyhedron $\tilde{R}_q^{\tau t}$ of operation τ of task t.

Some operations τ may encounter physical obstacles that arise during processing (e.g., activities involving the internal/external surfaces of products such as working inside an object's area with a furniture door opened). An obstacle obstructs the operator movements by preventing the occupation of colliding positions in S, and the execution of tasks by impeding their fulfillment whenever it interposes between the operator and the task. Let $\mathcal{L}_i^t \subseteq S$ be the parallelepiped-shaped region identifying the feasible feet center positions according to the obstruction induced by the i-th obstacle on all operations τ of task t, formally $\mathcal{L}_i^t = \{\mathbf{w}^t \in S : \mathbf{l}_i^t \leq \mathbf{w}^t \leq \mathbf{L}_i^t\}$. The continuity of the region is assumed due to the specificity of the considered cases as each task prescribes only one product's surface, among the internal and external, on which operations must be performed. We indicate with $\mathcal{L}^t$ the collection of regions related to the obstacles occurring during task t.

Operator's feet center positions during processing task t are described by the decision variables $\mathbf{w}^t \in S$, with $w_z^t = w_z$ for all the tasks. Binary variables σ_q^t describe the task's risk level: $\sigma_q^t = 1$ if task t is done with risk level $q \in Q \cup \{high\}$.

3.3.1. Constraints

The membership of a feet center in a risk polyhedron is modeled by the continuous variables $\lambda_{kq}^{\tau t}$, with $k = 1, \dots, m$, indicating the coefficients of the convex combination of vertices in $V_q^{\tau t}$. Convexity is enforced by setting

$$\sum_{k=1}^{m} \lambda_{kq}^{\tau t} = 1 \quad \forall t \in T, \tau \in I^t, q \in Q \tag{2}$$

$$\lambda_{kq}^{\tau t} \geq 0 \quad \forall t \in T, \tau \in I^t, q \in Q, k = 1, \dots, m \tag{3}$$

The feet center $\mathbf{w}^t$ for a task t is at low-risk level if for each operation $\tau \in I^t$, the point $\mathbf{w}^t$ belongs to the risk polyhedron $\tilde{R}^{\tau t}_{low}$, i.e., if

$$\mathbf{w}^t = \sum_{k=1}^{m} \lambda^{\tau t}_{k,low} \cdot \mathbf{v}^{\tau t}_{k,low} \qquad \forall t \in T, \tau \in I^t \tag{4}$$

Because the projections of $\tilde{R}^{\tau t}_{free}$ and $\tilde{R}^{\tau t}_{low}$ along S_{xy} are concentric and $\tilde{R}^{\tau t}_{free}$ is contained in $\tilde{R}^{\tau t}_{low}$, a feet center falling into $\tilde{R}^{\tau t}_{free}$ can be described as a point of $\tilde{R}^{\tau t}_{low}$ translated by a suitable $\boldsymbol{\delta}^{\tau t}$

$$\mathbf{w}^t + \boldsymbol{\delta}^{\tau t} = \sum_{k=1}^{m} \lambda^{\tau t}_{k,free} \cdot \mathbf{v}^{\tau t}_{k,free} \qquad \forall t \in T, \tau \in I^t. \tag{5}$$

Notice that constraints (4) and (5) force the point $\mathbf{w}^t$ to belong respectively to the set $\tilde{R}^t_{low}$ and $\tilde{R}^t_{free}$, the former (the latter) given by the intersection of all the risk polyhedra $\tilde{R}^{\tau t}_{low}$ ($\tilde{R}^{\tau t}_{free}$) of operations τ associated with the task t. This is why the operator is allowed to change position only between different tasks. Clearly, $\tilde{R}^t_{low}$ and $\tilde{R}^t_{free}$ still are polyhedra, we call them the low-risk and the free-risk polyhedron of task t, and $\tilde{R}^t_{free} \subseteq \tilde{R}^t_{low}$.

The membership of $\mathbf{w}^t$ to $\tilde{R}^t_{low} \setminus \tilde{R}^t_{free}$ can be established by the binary variable σ^t_{low} and the activation constrains

$$-B\sigma^t_{low} \le \boldsymbol{\delta}^{\tau t} \le B\sigma^t_{low} \qquad \tau \in I^t \tag{6}$$

where B is a large enough coefficient chosen to bound the maximum distance between any two points belonging to polyhedra of different risk levels.

Since low-risk levels are much more expensive than free-risk ones, it is not convenient to express a feet center belonging to $\tilde{R}^{\tau t}_{free}$ as $\mathbf{w}^t + \boldsymbol{\delta}^{\tau t}$ with $\boldsymbol{\delta}^{\tau t} \neq \mathbf{0}$, because $\boldsymbol{\delta}^{\tau t} \neq \mathbf{0}$ implies that $\sigma^t_{low} = 1$. Therefore, if the feet center $\mathbf{w}^t$ belongs to both $\tilde{R}^{\tau t}_{free}$ and $\tilde{R}^{\tau t}_{low}$ then $\boldsymbol{\delta}^{\tau t} = \mathbf{0}$. If, otherwise, $\mathbf{w}^t$ belongs to $\tilde{R}^{\tau t}_{low} \setminus \tilde{R}^{\tau t}_{free}$, a translation $\boldsymbol{\delta}^{\tau t}$ is necessary to move it into $\tilde{R}^{\tau t}_{free}$, but such a translation triggers the variable σ^t_{low} to assume the value 1, indicating that the feet center is at low-risk level. Finally, the constraints

$$\sigma^t_{free} + \sigma^t_{low} = 1 \qquad \forall t \in T \tag{7}$$

ensure that exactly one risk level is assigned to each task.

Further boxing constraints are introduced to address the presence of the obstacles in $\mathcal{L}^t$:

$$\mathbf{l}^t_i \le \mathbf{w}^t \le \mathbf{L}^t_i \qquad \forall t \in T, \mathcal{L}^t_i \in \mathcal{L}^t \tag{8}$$

Example 3.1. *Let us consider a product with origin in* $(0,0,0)$ *of dimensions* $60 \times 57 \times 30$ cm^3. *A touch task* t *requires the evasion on a hinge located on the internal left side of the product, that is the tolerance area's origin is in* $(s^t_x, s^t_y, s^t_z) = (0, -5, 10)$ *with variations* $(\epsilon^t_x, \epsilon^t_y, \epsilon^t_z) = (5, 15, 10)$. *Assume moreover that the product's door is opened to operate. The door can be physically identified as a horizontal parallelepiped with bottom-left-front corner in (0,-30,0) and sizes (60,30,5). Given the product's surface of interest (internal) and the open door, the corresponding obstruction-free region* $\mathcal{L}^t_1$ *defines bounds on the operator position on the* S_{xy} *plane as follows*

$$s^t_x + \epsilon^t_x = 5 \le w^t_x \quad , \quad w^t_y \le -30 \tag{9}$$

whereas other coordinates of $\mathbf{l}$ *and* $\mathbf{L}$ *are set to trivial lower and upper bounds, respectively.*

Note that, as alternative method, one can directly preprocess the shape of risk polyhedra by computing the intersection with obstacle hyperplanes. Vertices in $V^{\tau t}_q$ should then be generated accordingly. Nevertheless, we preferred relying on solver to manage the intersection with hyperplanes and keep the identification of vertices straightforward.

When the risk polyhedra of two (or more) concurrent operations in I^t do not intersect, meaning that there is either no unique worker position to fulfill both operations (e.g., fastening two hinges on opposite sides) or that the original tolerance region of an operation $\tau \in I^t$ is too large (e.g., cleaning a product side that is too tall), both $\tilde{R}^t_{low}$ and $\tilde{R}^t_{free}$ are empty. This implies that neither the risk-free nor the low-risk level can be assigned to the task t. In such cases, the task is marked as *high* risk. The high-risk level can be included in the integer program by adding the type $\{high\}$ to the set Q and setting the high-risk polyhedra as the feasible space S. Additionally, constraints (2)–(8) must be extended by introducing $V^{\tau t}_{high}$ sets, $\lambda^{\tau t}_{k,high}$ and σ^t_{high} variables, and $\boldsymbol{\rho}^{\tau t}$ as the analog of $\boldsymbol{\delta}^{\tau t}$ for moving into high-risk polyhedra.

However, preprocessing can alternatively be done, since each task t can be classified as high-risk in advance by directly looking at its risk polyhedron $\tilde{R}^t_{low}$, whose emptiness can be checked by the feasibility of the relevant constraints (2)–(5), or by specialized functions, e.g., in Python. If $\tilde{R}^t_{low}$ is empty, the relevant constraints (2)–(5) and variables $\lambda^{t\tau}_{kq}$ are dropped from the integer program, the cost of the task is set to $c_{high} \gg c_{low}$, and the feet center is set to the middle x-position and closest y-position positions between the operations in I^t. Specifically, $w^t_x = \frac{1}{2}(\max_\tau s^\tau_x - \min_\tau s^\tau_x)$, and $w^t_y = \min_\tau s^\tau_y$, with $\tau \in I^t$. The w^t_z coordinate is left free to take the value assigned by the program.

Preliminary experiments have shown that the precise modeling of the high-risk level with additional variables and constraints results in only marginal differences in feet center positions compared to preprocessing, albeit at the cost of non-negligible additional computational effort. Therefore, computational experiments have been conducted using preprocessing.

As a final consideration, the integer program can also be enhanced with constraints that address scenarios where product repositioning is performed by means of machine movements. Let us introduce a pair of vector variables $\mathbf{u}^t_+, \mathbf{u}^t_- \in R^3_+$ for each task $t \in T$ except the last one, indicating the increasing/decreasing translation of the product performed by the machine at the end of task t. Constraints (5), and similarly (4), are modified as follows:

$$\mathbf{w}^t + \boldsymbol{\delta}^{\tau t} = \sum_{k=1}^{m} \lambda^{\tau t}_{k,free} \cdot \mathbf{v}^{\tau t}_{k,free} + \sum_{j=1}^{t-1} (\mathbf{u}^j_+ - \mathbf{u}^j_-) \qquad \forall t \in T, \tau \in I^t \tag{10}$$

The summation on $\mathbf{u}$ variables expresses all the product translations occurred until the end of the previous tasks. Bounds can be inferred to limit $\mathbf{u}^t_+, \mathbf{u}^t_-$ values so that the positions fall within points reachable by the handling machine. The modified constraints ask position $(\mathbf{w}^t + \boldsymbol{\delta}^{\tau t})$ to belong to the translated risk polyhedron.

Fixed setup costs b for product repositioning can also be accounted in the integer program by defining binary variables u^t and adding constraints $\mathbf{u}^t_+ + \mathbf{u}^t_- \le M u^t$ where M a sufficiently large constant. Then, the total setup cost is given by $b \sum_{t=1}^{|T|-1} u^t$. In our setting, however, we assume $b \to \infty$ to prevent product repositioning.

3.3.2. Objective functions

The objective functions were formulated to capture the essential metrics for an approximate, off-the-shelf evaluation of the REBA risk index, that is, without the use of IoT devices, while ensuring the computational viability of the decision-support module. An optimal product-operator positioning minimizes the weighted total ergonomic cost C collected throughout all the tasks:

$$\min C = \sum_{t \in T} \sum_{q \in Q} d^t c_q \sigma^t_q. \tag{11}$$

Each task is weighted by its duration d^t. Moreover, ergonomic cost coefficients c_q are used with values $c_{free} = 1$ and $c_{low} = \max_{t \in T}\{d^t\}$, in order to make risk-free positions always preferred on low-risk ones.

Equivalent solutions typically exist because the ergonomic costs do not discriminate between different positions having the same ergonomic risk level. The ties are resolved in favor of feet center positions w^t closer to the worker's preferences, as described by the historical operator's postural habits $\mathbf{h}^t = (h^t_x, h^t_y, h^t_z)$. Therefore, an additional objective function

minimizes the weighted Euclidean distance H between the positions proposed by the model and the worker's historical preferred ones:

$$\min H = \sum_{t \in T} d^t \|\mathbf{h}^t - \mathbf{w}^t\|_2. \tag{12}$$

The discretization of the level of risk into free- low- and possibly high-risk zones introduces step discontinuities near the edge of the zones, where small movements cause large ergonomic costs variations (the feet center could be positioned at the boundaries of a lower-risk zone, therefore resulting ergonomically advantageous, even if it is very close to the a higher-risk zone). The step discontinuities can be smoothed by introducing a third optimization criterion that minimizes the Euclidean distance D between the feet center and the origins of operations:

$$\min D = \sum_{t \in T} d^t \sum_{\tau \in I^t} \|\mathbf{s}^\tau - \mathbf{w}^t\|_2. \tag{13}$$

Let $\bar{\mathbf{s}}$ the median point of the origins of operations in I^t, i.e., $\bar{\mathbf{s}}$ is such that $\sum_{\tau \in I^t} \|\mathbf{s}^\tau - \bar{\mathbf{s}}\|_2 = 0$. Thanks to (13), $\mathbf{w}^t = \bar{\mathbf{s}}$ if either $\bar{\mathbf{s}} \in \tilde{R}^t_{free}$ or $\bar{\mathbf{s}} \in \tilde{R}^t_{low}$ and $\tilde{R}^t_{free}$ is empty. If otherwise $\bar{\mathbf{s}} \in \tilde{R}^t_{low}$ and $\tilde{R}^t_{free}$ is not empty then $\mathbf{w}^t$ will be on the border of $\tilde{R}^t_{free}$. Clearly, this behavior does not apply if the risk polyhedra of tasks are arbitrary sets.

Finally, the product-operator positioning is also evaluated in terms of the operator's moves throughout the whole process, as ergonomic performance typically deteriorates for increasing distance traveled. Therefore, the total length L traveled by the worker is considered as the fourth minimization criterion:

$$\min L = \sum_{t \in T \setminus \{1\}} \|\mathbf{w}^t - \mathbf{w}^{t-1}\|_2. \tag{14}$$

Hierarchical multi-objective optimization problems can be addressed using the lexicographic approach Ehrgott (2005). Given the priority order $C \prec H \prec D \prec L$ of the objective functions, a lexicographic optimal solution is computed by solving successive optimization problems, each incorporating constraints that preserve optimality with respect to higher-priority objectives.

3.4. Preprocessing of quota's coordinates

The optimization model can be simplified by preprocessing the z-coordinates of the feet centers and then projecting the risk polyhedra to the plane S_{xy}.

Recall that w^t_z indicates the feet center quota in the employed reference system. The impact on the total ergonomic cost C of fixing w^t_z of a task t at a given value $\tilde{z}$ depends on whether $\mathbf{w}^t$ falls into the risk-free or low-risk polyhedron of the task t.

If t is a touch task, such impact only depends on the projection onto the S_{xy} plane of the risk polyhedra, since such a projection does not change for any fixed $\tilde{z}$ (for a single operation, it is a constant semicircle, see Fig. 5). Therefore, the optimal quota $\tilde{z}$ can be determined based only on whether the resulting quotas of the origins of all the operations in I^t fall between the operator's elbow and shoulder (risk-free level) or thigh and eye (low-risk level), or possibly outside these ranges (high-risk level).

Otherwise, if t is a vision task, the projections onto the S_{xy} plane of its risk polyhedra change with the quota $\tilde{z}$, becoming smaller when w^t_z moves farther from $\tilde{z}$ (we recall that the risk polyhedra of a single operation are pseudo-cones). In this case, the emptiness of the projections onto the S_{xy} plane is evaluated for different step-wise values of $\tilde{z}$ (1 cm in our experiments), and the highest quota with the most convenient risk-level non-empty projection is chosen. Ties among different coordinates are resolved by evaluating subsequent criteria H and D, limited to the z-axis.

Differently from the preprocessing of the high-risk tasks described in Section 3.3.1, the above procedure also fixes the quota of high-risk tasks. To avoid influencing the selection of $\bar{w}_z$ by considering tasks whose ergonomic risk is unavoidably compromised, i.e., those resulting in high risk for any $\tilde{z}$, the quotas of such tasks are left unfixed in the integer program.

Table 2
Characteristics of products used for the experimentation.

Product	Typology	Width (x) [cm]	Depth (y) [cm]	Height (z) [cm]
P1	Drop-down	120	33	36
P2	Drop-down	60	57	30
P3	Standard 2 doors	90	45	72
P4	Drop-down	45	45	96
P5	Drop-down	30	33	72
P6	Standard 1 door	60	33	72
P7	Standard 2 doors	80	33	96

4. Experiments and results

4.1. Experimentation procedure

The proposed approach proves to be particularly suitable for implementation in manufacturing environments characterized by a wide range of highly diverse products, substantial and bulky dimensions, the need to perform various tasks on the same product in different zones, a clear prevalence of manually performed activities, and the presence of operations that require significant physical effort.

Specifically, the case study has been derived from a real-world industrial scenario: a manual workstation for assembling kitchen cabinets at LUBE Industries, a leading kitchen manufacturer in Italy[3]. In the as-is workstation configuration, manual activities, such as front panel assembly, shelf insertion, and cleaning, are carried out with the cabinet fixed over a conveyor belt. Variations in worker anthropometrics lead to awkward and uncomfortable postures due to the fixed product position, resulting in medium-high overall ergonomic risks, presenting distinct challenges for different operators.

The optimization model has been tested in a Virtual Reality (VR) environment using Siemens Tecnomatix Process Simulate. Through the integration of HTC Vive PRO with Tecnomatix Process Simulate, users are immersed in the VR environment, enhancing the simulation process. This approach not only facilitates the testing process but also allows for greater customization and flexibility in experimental setups. To ensure the validity and robustness of the experiments, 7 products corresponding to as many distinct products were carefully selected, each characterized by distinct dimensions, a diverse range of door-opening mechanisms, and different tasks. This meticulous selection aimed to encompass a broad spectrum of real-world scenarios, thereby enhancing the representativeness of the findings. Table 2 provides a detailed overview of the product characteristics.

Various tasks were defined for each product covering different areas and functionalities. For each task, the type (vision or touch), origin, and extent of the tolerance zone were specified. Additionally, constraints (obstacles) that come into effect following specific tasks were also defined. For example, the door-opening task triggers a constraint as it creates a plane (that of the door) that restricts the operator's movements. Fig. 7 presents the tasks list for product 4 and the relative definition of tolerance zones.

For the test, three male and three female were selected, with heights ranging from the 5th to the 95th percentile of the ANSUR II database Gordon et al. (2014). This selection aims to capture a diverse range of heights within the general population, facilitating the verification of the model's effectiveness on a representative sample. Table 3 displays the anthropometric characteristics of the users.

Each task was performed with products in three different workplace configurations:

1. Fixed position (as-is industrial scenario) (F): the product was placed on the workbench at a height of 70 cm.

[3] https://www.cucinelube.it

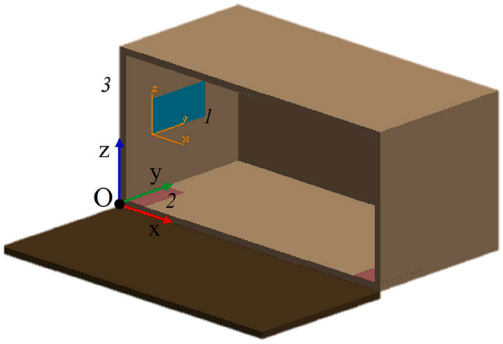

Task			Task coordinates relative to the product origin	
			Origin (x;y;z)	*εx; εy; εz*
1	Inspect internal label on the left	Vision	0;10;18	5;20;10
2	Adjust internal mechanisms on the left (red area)	Touch	5; 0; 0	10;15;10
3	Remove external label and clean on the left	Touch	-10;0;0	10;45;45

Fig. 7. Tasks descriptions and areas definition for product 4.

Table 3
User anthropometric characteristics.

User	Gender	Stature	Eye H.	Shoulder H.	Elbow H.	Fingertip H.
1	F	163	148	135	101	66
2	F	155	143	128	96	58
3	F	172	162	141	110	70
4	M	173	161	146	104	63
5	M	183	172	155	117	69
6	M	191	183	166	123	74

2. Operator's preferred position (P): The user moves the product and selects its preferred position (based on the product and task) to ensure the activity is as comfortable as possible. The corresponding product coordinates were measured with respect to the reference-system origin and used to quantify the operator's preferred position as a personalized input to the optimization model.
3. Position computed by the integer program (O): The product was positioned according to the results obtained by the optimization model.

Before starting the test, users familiarized themselves with the headsets and selected their preferred positions for each product. Thanks to VR, users were able to move the product easily and quickly until they found the most comfortable position for them. It was possible to define a unique height for each product, while a different position on both the x and y axes was allowed for each task. Since the tests were conducted in a virtual environment, the preferred product position was directly measured in Tecnomatix Process Simulate.

During the test, participants wore 17 inertial motion capture sensors (Xsens MVN) for full-body kinematic tracking (Fig. 8). The system records movement data and exports joint angles, allowing for precise and objective analysis of posture and motion across all frames. These data were used to assess biomechanical and postural loads, using the REBA method Hignett and McAtamney (2000), which evaluates individual workers' exposure to the risk of MSDs in both upper and lower limbs. The REBA method has been automated through specific algorithms that process sensors data, compute scores for various steps, and derive the final risk index.

4.2. Results of the optimization approach

Convex mixed-integer optimization problems are well known to belong to the class of NP-hard problems, meaning that, generally speaking, efficient algorithms for their exact solution are unlikely to exist. Nevertheless, from an experimental standpoint, the results reported below indicate that optimal or near-optimal solutions for realistic instances can be obtained within reasonable computation times, thereby demonstrating the practical applicability of the proposed method.

Experiments involving the optimization approach were run on a machine equipped with a processor Intel® Core™ i7-7500U (2 cores) 2.90 GHz with 16Gb RAM. Preprocessing phase was coded using Python 3.7.0. The convex integer program was implemented with AMPL and solved by Octeract Engine 4.6.0, which exploit parallel branch-and-bound invoking IBM CPLEX 22.1.1.0 for the integer linear subproblems. A time limit of 1200 seconds was set in each iteration of the lexicographic approach. The unit measure for space S description was cm, also employed as step in the preprocessing procedure, and parameter c_{high} was set equal to 100.

Table 4
Features of the products relevant for the optimization model.

Product	$\|T\|$	$\|I\|$	#vision	$\|\mathcal{L}\|$	$\bar{d}$
1	5	7	0	3	2.8
2	5	7	0	3	2.8
3	7	10	0	0	2.0
4	3	3	1	0	4.7
5	3	3	1	0	4.7
6	4	4	1	0	5.0
7	4	4	1	0	5.0

Table 5
Average results per product.

Product	$\bar{r}_{free}$	$\bar{r}_{low}$	$\bar{r}_{high}$	$\bar{C}$	$\bar{H}$	$\bar{D}$	$\bar{L}$	$\bar{RT}$
1	0.20	0.60	0.20	236.00	495.92	1669.12	110.64	3.98
2	0.40	0.60	0.00	38.00	395.94	1400.75	81.85	17.95
3	0.29	0.67	0.05	267.00	275.34	1948.62	139.64	974.63
4	0.67	0.33	0.00	44.00	542.66	1303.50	41.85	6.73
5	1.00	0.00	0.00	14.00	616.04	1036.96	48.67	0.67
6	0.00	1.00	0.00	100.00	556.59	2257.47	109.94	8.60
7	0.00	0.63	0.38	812.50	658.65	1959.07	134.23	8.19

For each product, Table 4 shows the number of task, the number of operations, that is $|I| = \sum_{t\in T} |I^t|$, and the number of obstacles, given by $|\mathcal{L}| = \sum_{t\in T} |\mathcal{L}^t|$. Moreover, the number of vision tasks and the mean task duration $\bar{d}$ are listed.

Table 5 reports, for each product, the average measures computed among the users. The index $\bar{r}_q$ for $q \in \{free, low, high\}$ indicates the mean fraction of task performed with a level of risk q. Columns 4–8 give the mean values of criteria (11)–(14). The last column shows the average running time $\bar{RT}$ (in seconds) spent by the solver to perform the entire lexicographic approach. Analogous data are reported in Table 6 for each user by averaging over the products.

Except for product 5 (P5), all the products exhibit a relevant fraction of the tasks completed with at least low risk, see Table 5. The mean ergonomic cost $\bar{C}$ appears more pronounced for products 1, 3 and 7 due to the presence of tasks performed under high risk. In the first case, the high risk depends by the distance along the x axis among two hinges on the opposite sides of the product. Being the Golden zone independent by the user's anthropometric characteristic, this outcome is common to all the users. For the other products instead, tasks located at the floor and top of the products ask the user to span a sufficiently extended Strike

Fig. 8. Users during the experimentation.

Table 6
Average results per user.

User	$\bar{r}_{free}$	$\bar{r}_{low}$	$\bar{r}_{high}$	$\bar{C}$	$\bar{H}$	$\bar{D}$	$\bar{L}$	$\bar{RT}$
1	0.36	0.51	0.12	303.57	498.68	1627.18	101.00	206.90
2	0.36	0.51	0.12	303.57	445.88	1641.05	117.92	182.35
3	0.36	0.54	0.10	223.00	586.12	1639.45	106.07	68.61
4	0.39	0.51	0.10	222.64	524.54	1637.13	84.69	26.85
5	0.36	0.57	0.06	155.14	449.87	1683.32	86.52	175.70
6	0.34	0.63	0.03	87.64	530.17	1693.72	75.36	214.52

zone, which depends by the user's characteristics, to allow the completion of all these tasks within low risk. Specifically, only users from 3 to 6 on P3, and users 5 and 6 on P7 are satisfying this requirement. This phenomenon, along with the dependence of the Field of View by the user's height, explains the reduction in the ergonomic costs for taller users, see Table 6.

In general terms, the variability among ergonomic results appear limited among different users and, for P2 and P6, among different tasks. This suggests that the current method, although being able to provide a measure of the risk compliant with the ergonomic principles, can potentially be further improved by considering an user-dependent Golden zone, and a refined risk scale in the model of inter-level risks in addition to *free, low* and *high*.

While it is hard to detect a pattern in the distances $\bar{H}$ from user-preferred positions, the measures of distance $\bar{D}$ from tasks and user travelled length $\bar{L}$ appear positively correlated to the products' width.

Concerning the performance of the optimization model, a total CPU time of 6142.5 seconds was spent to run the lexicographic approach on all user-product pairs. However, 95.6 % of the time was required to solve the instances with P3, whereas the mean running time on all the other user-product pairs was 7.7 seconds. The practical difficulty on P3 can be possibly ascribed to the number and peculiarity of the tasks involved. Time limits occurred for users 1, 2 (criterion L), 5 and 6 (criterion H). The optimality gap was on the mean 0.64 % among the first three users and the last did not found a dual bound to prove the optimality of the current solution.

Fig. 9 shows the reduction of the optimality gap over time for the D and L criteria in the P3-User1 instance (the curves for C and H are not reported due to the negligible running time of the corresponding optimization steps). For both criteria, the convergence pattern is typical of hard combinatorial problems: effective feasible solutions are identified very quickly, after 1.1 seconds for D and 4 seconds for L, while the remaining running time is spent improving the dual bounds to certify optimality. For the D criterion, the optimality gap drops to 1.17 % after just 2.1 seconds within a total running time of 235 seconds required by the step. Beyond this point, convergence slows and the curve exhibits a plateau. A similar trend is observed for the L criterion: the optimality gap reaches 3.08 % after 27.1 seconds, after which the solver enters a plateau phase that lasts until the time limit, ultimately resulting in a final gap of 1.01 %.

Table 7
Percentage reduction in REBA score and step count between fixed (F) and optimized (O) configurations for each product. Negative values indicate an increase in ergonomic risk or movements.

Product	REBA reduction	Step reduction
P1	26 %	100 %
P2	33 %	0 %
P3	0 %	0 %
P4	36 %	58 %
P5	34 %	-15 %
P6	10 %	19 %
P7	13 %	33 %

The described behavior, and evidences from the full test-bed, suggest a weakness on the dual bound side of the formulation, while (optimal) primal solutions are usually computed in short time. Interestingly, the introduction of obstacles seems to have no significant effect on the running times.

Finally, the lexicographic approach exhibited an uneven distribution of the computational burden: in order, optimizing criterion C demanded only 5.8 % of the total time, H asked for 27.8 %, then D accounted for 18.1 % and L for the remaining 48.5 %. It is worth noting that, on the average, the final step of the approach improved L by 18.1 % while worsening criterion D of only 1.04 %.

4.3. Ergonomic results

As illustrated in Fig. 10, the aggregated analysis across all products indicates that position optimization generally leads to improved ergonomic conditions. Specifically, Table 7 reports the percentage reduction in REBA score and step count between the fixed and optimized configurations for each product, showing a mean reduction of 22 %. Step count was also evaluated as an indicator of unnecessary movements, an ergonomic inefficiency known as *muda* in Lean philosophy, typically measured through step counting.

For all products, with the exception of product P3, the fixed configuration was identified as the most ergonomically hazardous. The most pronounced improvements were observed for compact products (P1, P2, P4, and P5), where task areas were spatially concentrated, allowing the mathematical model to identify optimal operator-product positions. For P2 and P3, the step reduction was 0 % because no steps were recorded

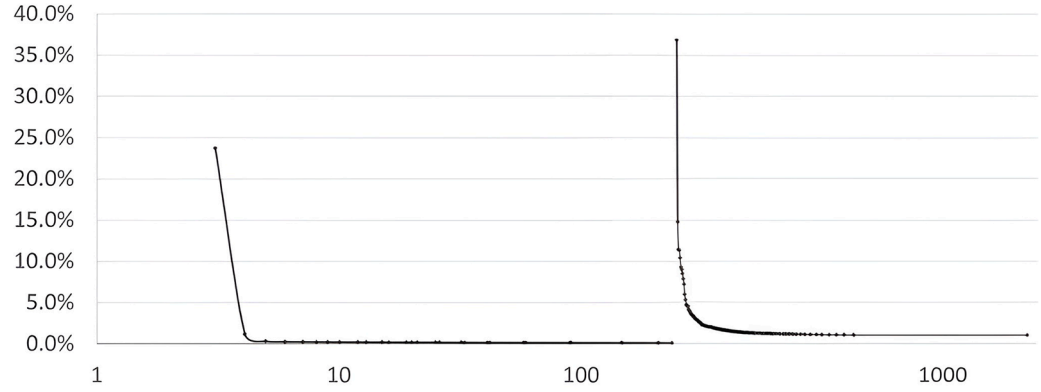

Fig. 9. CPU running time (in logarhitmic scale) vs. optimality gap of P3-User1 instance, for the subsequent optimization of D and L criteria..

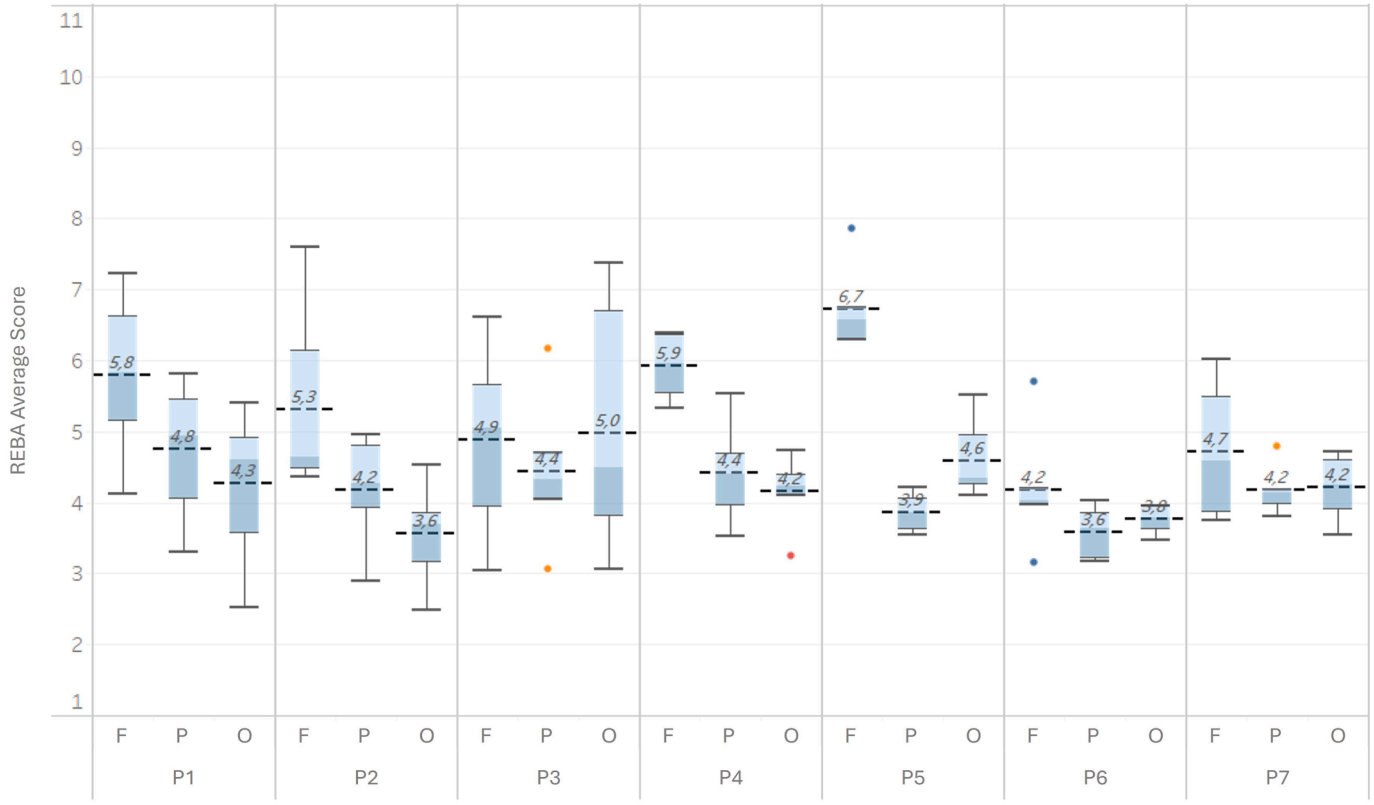

Fig. 10. REBA average score for each workplace configuration and product. The average score for each product and each configuration is displayed with a dashed line.

in either configuration, indicating that all tasks were performed from a static position. Whereas, P5 displayed a slight increase in step count despite a marked REBA reduction, possibly reflecting user repositioning to improve task visibility or accessibility. P3 did not benefit from optimization, likely due to its large size and the wide spatial separation of task zones, which limited the model's ability to maintain an ergonomic position throughout the activity. Larger products (P6 and P7) also showed smaller improvements, mainly due to the distribution of work areas on multiple sides of the product, which constrained the definition of a single optimal position.

When comparing the optimized and preferred configurations, results show a generally comparable level of ergonomic benefit in terms of REBA scores. In some cases (P5 and P7), users' preferred positions achieved slightly lower REBA values, suggesting that personal experience and habitual posture can lead to configurations close to the model optimum. However, step count analysis revealed that these preferred positions often required more movement, indicating that user comfort does not necessarily correspond to movement efficiency. Conversely, the optimized configuration systematically minimized operator displacement while maintaining low REBA values, thus representing the best compromise between posture and task efficiency.

The percentage variations in REBA scores among users demonstrated a diverse range of responses to optimization. Some users benefited from significant reductions, such as User5 with 33 % and User1 with 28 %, while others showed more modest changes, like User4 with 13 %. This underscores the importance of considering individual preferences and anthropometric characteristics when implementing ergonomic solutions. Fig. 11 illustrates, for P2, the distribution of time spent in each REBA risk category across users and configurations, confirming a marked shift toward lower-risk postures in the optimized setup.

From a risk management perspective, it is also important to examine worst-case scenarios, namely the product-user combinations for which

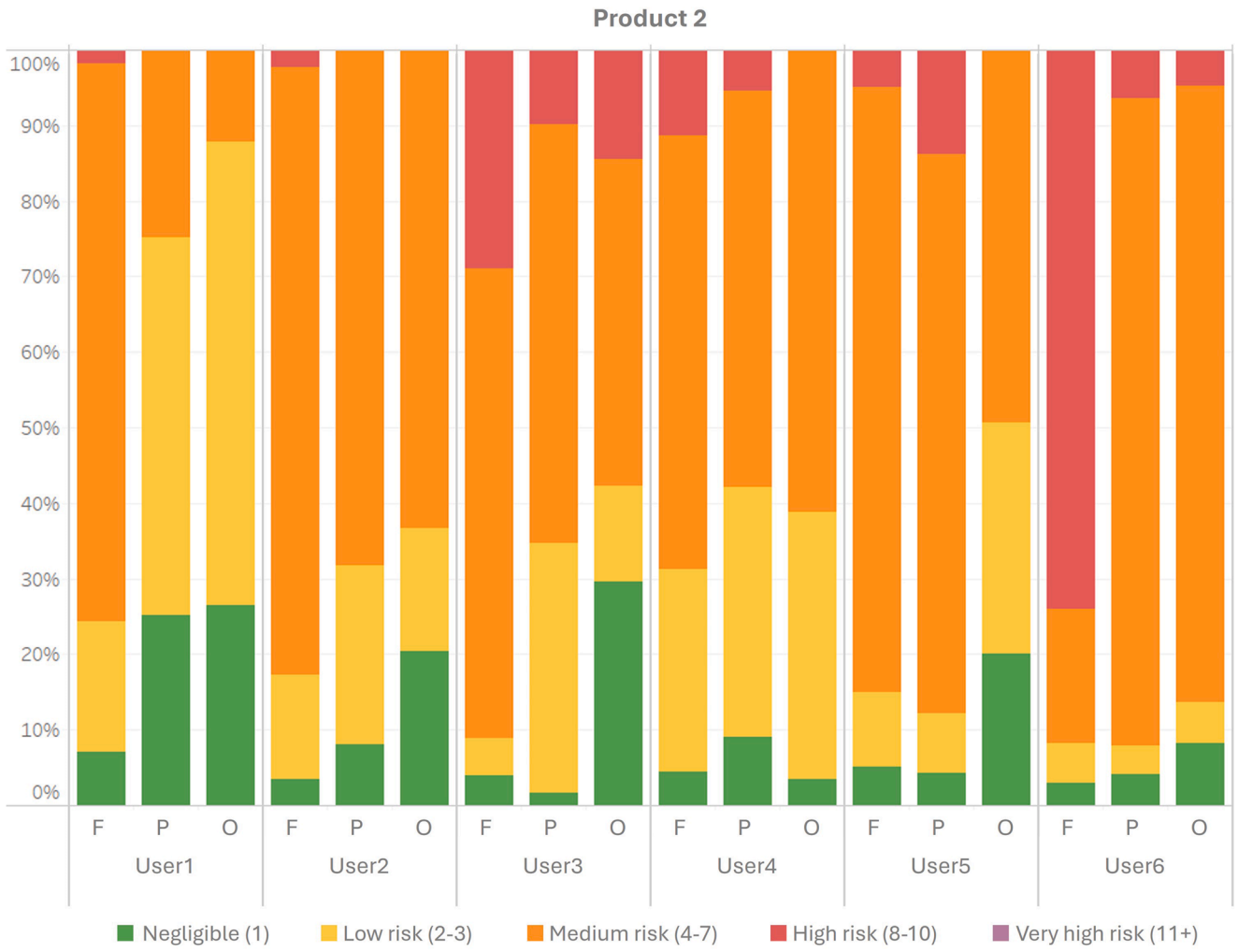

Fig. 11. REBA score for P2.

the optimized solution yields the highest percentage of time spent in the high-risk REBA category for each product and for each user (see Fig. 12). This analysis provides additional insight into the conditions under which optimization may be less effective or where individual adjustments are most needed. With the exception of combinations P3-User2 and P7-User1, the ergonomic profile obtained from the model solution is always better than the fixed configuration. Moreover, in three cases (P1-User3, P6-User6 and P7-User5), the solution generated by the proposed approach is even better than the preferred-position configuration.

A Linear Mixed Model (LMM) was employed to investigate the relationship between the REBA risk index and the three workplace configurations. LMM considered user and product as random effects, and configuration and side (dominant/ non-dominant) as fixed effects. All analyses used Holm's correction for multiple comparisons. The LMM revealed a highly significant overall effect of configuration on REBA scores ($F = 53.91$, $p < 0.001$). Specifically, post-hoc comparisons showed that the optimized configuration significantly reduced the REBA score compared to the fixed one (mean difference = 1.17, $p < 0.001$). Similarly, the preferred configuration also resulted in a significant REBA reduction relative to the fixed one (mean difference = 1.20, $p < 0.001$). There was no statistically significant difference in REBA scores between the optimized and preferred configurations (mean difference = 0.02, $p = 0.874$). Furthermore, a significant effect of side was observed ($F = 6.86$, $p = 0.009$), while the interaction between configuration and side was not significant, indicating the configuration's impact is consistent across both sides. These findings robustly demonstrate that transitioning from a fixed setup to an optimized configuration significantly lowers ergonomic risk, with the optimization model achieving a comparable level of ergonomic benefit to that preferred by users.

To analyze individual product performance, separate LMMs were run for each product (Table 8). These models included configuration, side, task, and their interactions as fixed effects, with user as a random effect. The analysis consistently showed highly significant effects for configuration (all $p \leq 0.005$) and task (all $p < 0.001$) on REBA scores across all products. The side effect was significant only for P4, P5, P6, and P7. Most fixed interactions were non-significant, indicating consistent configuration impacts, except for configuration * task in P7 ($p < 0.001$). Post-hoc comparisons confirmed that, for almost all products, both optimized and preferred configurations significantly reduced REBA scores compared to the fixed one. The comparison between optimized and preferred highlighted mixed results. For P4, P6, and P7, no significant difference was found, suggesting comparable ergonomic benefits. However, optimized significantly outperformed preferred for P1 and P2 ($p \leq 0.002$), while preferred significantly outperformed optimized for P3 and P5 ($p \leq 0.005$). These findings indicate that user preferences can also incorporate ergonomic factors not fully captured by geometric optimization alone.

To investigate individual differences, a separate series of LMMs was run for each user (Table 9).

These models included configuration, side, task, and their interactions as fixed effects, with product treated as a random effect. The

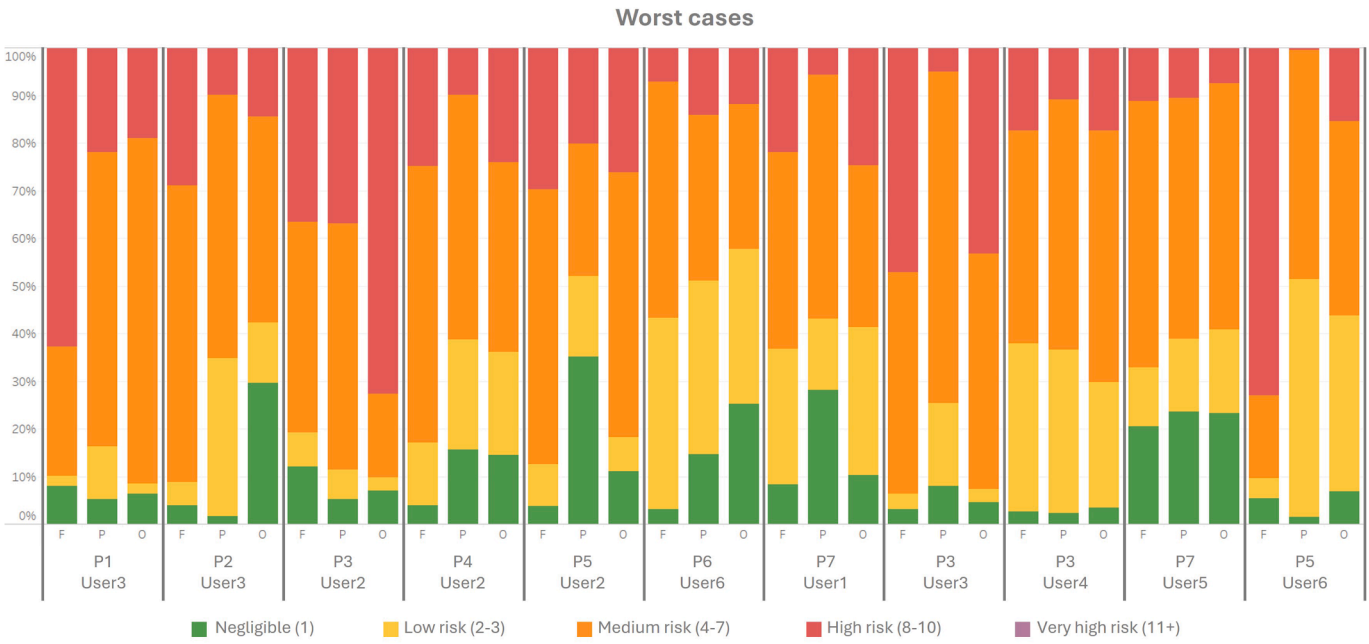

Fig. 12. Worst-case scenarios: highest REBA high-risk score per product and per user (User1's worst case is P7 and User2's worst case is P3).

Table 8
LMM results for REBA risk index in relation to workplace configurations (F: fixed, P: preferred, O: optimized) for each product.

Product	R^2 Marginal	R^2 Conditional	Configuration *p*-value	Side *p*-value	Task *p*-value	F - O (*p*-value)	F - P (*p*-value)	O - P (*p*-value)
P1	0.354	0.640	<0.001	0.759	<0.001	1.573 (<0.001)	0.987 (<0.001)	-0.586 (0.002)
P2	0.426	0.631	<0.001	0.984	<0.001	1.788 (<0.001)	1.165 (<0.001)	-0.622 (<0.001)
P3	0.391	0.720	0.001	0.809	<0.001	0.040 (0.825)	0.600 (0.004)	0.560 (0.005)
P4	0.577	0.638	<0.001	0.005	<0.001	2.160 (<0.001)	1.865 (<0.001)	-0.295 (0.225)
P5	0.687	0.689	<0.001	0.005	<0.001	2.240 (<0.001)	3.094 (<0.001)	0.854 (0.001)
P6	0.638	0.717	0.001	<0.001	<0.001	0.390 (0.027)	0.577 (<0.001)	0.187 (0.231)
P7	0.562	0.643	0.005	<0.001	<0.001	0.611 (0.014)	0.626 (0.014)	0.015 (0.945)

Table 9
LMM results for REBA risk index in relation to workplace configurations (F: fixed, P: preferred, O: optimized) for each user.

User	R^2 Marginal	R^2 Conditional	Configuration *p*-value	Side *p*-value	Task *p*-value	F - O (*p*-value)	F - P (*p*-value)	O - P (*p*-value)
U1	0.392	0.451	<0.001	0.253	<0.001	1.173 (<0.001)	1.056 (<0.001)	-0.117 (0.609)
U2	0.206	0.453	0.005	0.371	<0.001	0.748 (0.020)	0.895 (0.007)	0.147 (0.608)
U3	0.318	0.671	<0.001	0.076	<0.001	1.288 (<0.001)	1.512 (<0.001)	0.223 (0.363)
U4	0.359	0.461	0.002	0.386	<0.001	0.617 (0.005)	0.647 (0.004)	0.030 (0.882)
U5	0.410	0.471	<0.001	0.249	<0.001	1.132 (<0.001)	0.804 (0.001)	-0.328 (0.156)
U6	0.428	0.592	<0.001	0.244	<0.001	1.878 (<0.001)	1.577 (<0.001)	-0.301 (0.194)

analysis consistently showed a highly significant effect of configuration on REBA scores for all users (all $p \leq 0.005$), confirming its universal impact on ergonomic risk regardless of individual characteristics. Similarly, the task effect was highly significant for all users (all $p < 0.001$). The side effect and the fixed interaction terms were non-significant. Post-hoc comparisons further reinforced these conclusions. For all users, both optimized and preferred configurations led to statistically significant reductions in REBA scores compared to the fixed configuration. The comparison between optimized and preferred revealed significant equivalence at the individual level. For all users, no statistically significant difference was found between the two configurations. This strongly validates the model's practical applicability and its alignment with operator perceptions and needs.

5. Discussion

Results from experiments conducted in a laboratory reproducing real industrial conditions demonstrated the model's effectiveness in reducing ergonomic risk. Across all products, optimized configurations achieved an average 22 % reduction in REBA scores compared to fixed setups, confirming the capability of the proposed approach to enhance operator ergonomics through systematic workstation optimization. Optimized worker positioning led to significant improvements in ergonomic outcomes compared to fixed configurations, underscoring the critical role of systematic optimization based on ergonomic principles in mitigating workplace hazards and promoting worker health.

The ergonomic risks identified through the three-level risk scale of the optimization model, on average, provided a good approximation of the REBA scores obtained with the optimized configuration in the experiments. However, it is important to acknowledge that the REBA analysis utilized for the ergonomic assessment differs from the Golden and Strike Zone analysis considered in the model. The REBA analysis focuses on evaluating the ergonomic risks associated with body posture, force, type of movement, and repetition, providing a comprehensive assessment of musculoskeletal strain. On the other hand, the Golden and Strike Zone analysis emphasizes the optimal positioning of tasks and materials within the workspace. This fundamental difference in focus and methodology may contribute to the observed discrepancies between the

ergonomic analysis results and the model's outcomes. Notably, an unacceptable strike zone (red zone) may indicate a high risk for only a specific body part, such as the upper arm (step 7 of the REBA), without necessarily causing a significant increase in the overall risk index.

Beyond methodological differences, human variability also plays a key role in ergonomic outcomes. Despite instructing participants to replicate the same movements identically across all setups, slight deviations in posture or movement - due to fatigue, muscle memory, or unconscious adaptation - may have occurred. These small variations, though not related to the model, can influence REBA results. Acknowledging this inherent variability highlights the challenges of achieving perfect consistency in ergonomic assessments and underscores the importance of repeated trials or larger participant samples to ensure data reliability. The variability observed across different tasks and users further underscores the complexity of ergonomic optimization. Factors such as task complexity, workspace, design, and individual anthropometric characteristics influence the effectiveness of ergonomic solutions. Tailoring interventions to specific workplace conditions and user profiles remains crucial for achieving optimal outcomes. Overall, the results of the statistical analysis showed that transitioning from fixed workplace configurations to either optimized or preferred setups results in a significant reduction in the REBA risk index, with no significant difference observed between optimized and preferred overall.

Integrating ergonomic principles directly into the product-operator positioning process enables workplaces to significantly reduce the incidence of WRMSDs. The study's findings suggest that tailored ergonomic solutions based on individual worker characteristics lead to better overall ergonomic outcomes compared to fixed or user-preferred positions. Optimized product positioning not only enhances ergonomic conditions but also improves operational efficiency by minimizing unnecessary movements and task completion times. This benefit is particularly evident in products like P1 and P4, where optimized configurations resulted in substantial reductions in task steps. The use of a VR environment allowed for a detailed analysis of ergonomic performance across different user heights and workplace configurations in a controlled setting, ensuring the robustness and reliability of the experimental findings. Involving workers in defining ergonomic constraints and preferences fosters a sense of ownership and increases their commitment to adopt healthier work practices. This behavioral aspect is crucial for the long-term sustainability and acceptance of ergonomic interventions in industrial settings. Furthermore, the industrial adoption of ergonomically optimized solutions requires reskilling initiatives and human-centric design modules aligned with the Industry 5.0 training agenda (Gürdür Broo et al., 2022).

5.1. Limitations and future works

Despite its promising outcomes, the study also identified several challenges and areas for future research. Large products present limited flexibility for repositioning when tasks require working across multiple widely spaced areas. Consequently, a more detailed analysis of the movements performed by users during various tasks is advisable. The current study's limitation derives from conducting only a single repetition per configuration, which is insufficient when the variation in product-operator positions between configurations is minimal. This limitation is even more evident when REBA scores for the optimized configuration are less favorable than those for the user-preferred positions. This highlights that operator preferences often encompass a broader range of factors, such as overall comfort and workflow, that the REBA method captures. Nonetheless, the closeness of the optimized and preferred positions suggests that our model effectively accounts for user habits and natural working postures. To improve the robustness of the results and further refine the model, additional testing with multiple repetitions will be performed for each user, each product, and each configuration. This approach aims to mitigate the impact of variability in the movements performed and enhance the reliability of the results.

Looking ahead, several promising avenues for future research in ergonomic optimization within Industry 5.0 emerge. One potential enhancement involves introducing operator-dependent adjustments to the Golden Zone. This approach would offer *xy*-plane flexibility for tasks requiring manual interaction, thereby improving user comfort, efficiency, and overall ergonomic performance by accommodating individual anthropometrics and preferences. Another important direction for future research is expanding the model to incorporate some aspects of the REBA method. Specifically, integrating multiple risk levels into the model's framework, aligning with the REBA method's use of five levels rather than the current three, could be beneficial. This advancement would allow for a more detailed assessment of various ergonomic risk factors during work operations. However, implementing this enhancement presents significant challenges, particularly in accurately defining parameters for numerous risk areas, each of which would require specific boundaries and associated ergonomic metrics based on anthropometric data, biomechanics, and safety regulations.

Although the proposed optimization model was validated for industrial environments, it was conceived as a general approach for defining the optimal relative position between product and operator to minimize ergonomic risk. The method builds on a set of specific assumptions (e.g., ergonomic risk models, product types, and task characteristics) that can be reconfigured for different working settings. However, the extent to which these assumptions hold in other domains (e.g. tasks with different interaction modalities, products with highly variable geometries, or different workstation configurations) should be assessed through dedicated validation studies. For this reason, future work will need to test the proposed framework in a broader range of operational contexts, including sectors beyond assembly, such as logistics, healthcare, or construction, to confirm its generalizability and robustness. Validation in real production environments, especially in cells where collaborative robots support product positioning, will also be important to evaluate integration, safety, and human-robot interaction aspects.

Finally, integrating real-time feedback mechanisms into the optimization process represents another frontier for future development. Technologies such as vision-based systems could enable real-time ergonomic risk assessment, displaying REBA scores to workers for proactive safety management. This approach has the potential to enhance worker safety, productivity, and ergonomic compatibility. Conducting longitudinal studies to assess the long-term ergonomic impact of optimized product positioning is essential. Tracking health outcomes and ergonomic well-being over extended periods will validate the sustained effectiveness of the model in reducing WMSDs and improving overall workplace health.

6. Conclusions

This work presented an intelligent decision-support system for ergonomic workstation configuration that integrates anthropometric, task-related, and operational data into a multi-objective optimization framework. The experimental validation in a virtual industrial environment showed that positioning the product with respect to the operator through the proposed model can significantly reduce ergonomic risk, achieving on average a 22 % decrease in REBA scores compared with fixed configurations, while preserving operational efficiency. The comparison with user-preferred setups further indicated that the optimization model can reach ergonomic outcomes comparable to those intuitively selected by workers, but with a more consistent reduction of unnecessary movements. These results confirm the feasibility of embedding ergonomics into product-operator positioning as a proactive strategy for preventing WRMSDs in industrial contexts. The proposed framework can therefore support human-centric manufacturing initiatives by providing actionable set-points for machines and reconfigurable workstations. As Industry 5.0 continues to evolve, the integration of advanced robotics, simulation, and AI-driven solutions with ergonomic optimization models will be crucial. This convergence will further

enhance the adaptability, intelligence, and responsiveness of ergonomic interventions, fostering safer, more efficient, and human-centered manufacturing systems.

CRediT authorship contribution statement

Marianna Ciccarelli: Methodology, Formal analysis, Investigation, Resources, Data curation, Writing - original draft, Writing - review & editing, Visualization; **Michele Germani:** Writing - review & editing, Supervision; **Fabrizio Marinelli:** Conceptualization, Validation, Writing - review & editing, Supervision; **Alessandra Papetti:** Conceptualization, Methodology, Validation, Formal analysis, Investigation, Writing - original draft, Writing - review & editing, Visualization; **Andrea Pizzuti:** Conceptualization, Methodology, Validation, Formal analysis, Investigation, Writing - original draft, Writing - review & editing, Visualization.

Data availability

Data will be made available on request.

Declaration of competing interest

The authors declare that they have no known competing financial interests or personal relationships that could have appeared to influence the work reported in this paper.

References

Bautista, J., Batalla-García, C., & Alfaro-Pozo, R. (2016). Models for assembly line balancing by temporal, spatial and ergonomic risk attributes. *European Journal of Operational Research*, *251*(3), 814–829.

Busch, B., Maeda, G., Mollard, Y., Demangeat, M., & Lopes, M. (2017). Postural optimization for an ergonomic human-robot interaction. In *2017 IEEE/RSJ int. conference on intelligent robots and systems (IROS)* (pp. 2778–2785).

Ciccarelli, M., Papetti, A., Cappelletti, F., Brunzini, A., & Germani, M. (2022). Combining world class manufacturing system and industry 4.0 technologies to design ergonomic manufacturing equipment. *International Journal on Interactive Design and Manufacturing*, *16*, 263–279.

Dalle Mura, M., & Dini, G. (2019). Optimizing ergonomics in assembly lines: A multi objective genetic algorithm. *CIRP Journal of Manufacturing Science and Technology*, *27*, 31–45.

Dammacco, L., Carli, R., Lazazzera, V., Fiorentino, M., & Dotoli, M. (2022). Designing complex manufacturing systems by virtual reality: A novel approach and its application to the virtual commissioning of a production line. *Computers in Industry*, *143*.

De Kok, J., Vroonhof, P., Snijders, J., Roullis, G., Clarke, M., Peereboom, K., Pim, v. D., & Isusi, I. (2019). Work-related musculoskeletal disorders : prevalence, costs and demographics in the EU. https://doi.org/10.2802/66947

Ehrgott, M. (2005). Multicriteria optimization. Springer Berlin, Heidelberg.

El Makrini, I., Mathijssen, G., Verhaegen, S., Verstraten, T., & Vanderborght, B. (2022). A virtual element-based postural optimization method for improved ergonomics during human-robot collaboration. *IEEE Transactions on Automation Science and Engineering*, *19*(3), 1772–1783.

Eswaran, M., Inkulu, A. k., Tamilarasan, K., Bahubalendruni, M. V. A. R., Jaideep, R., Faris, M. S., & Jacob, N. (2024). Optimal layout planning for human robot collaborative assembly systems and visualization through immersive technologies. *Expert Systems with Applications*, *241*, 122465.

Gomes, W., Maurice, P., Dalin, E., Mouret, J.-B., & Ivaldi, S. (2022). Multi-objective trajectory optimization to improve ergonomics in human motion. *IEEE Robotics and Automation Letters*, *7*(1), 342–349.

Gordon, C. C., Blackwell, C. L., Bradtmiller, B., Parham, J. L., Barrientos, P., Paquette, S. P., Corner, B. D., Carson, J. M., Venezia, J. C., Rockwell, B. M., Mucher, M., Kristensen, S. (2014). 2012 Anthropometric survey of us army personnel: methods and summary statistics. Army Natick Soldier Research Development and Engineering Center MA, Tech. Rep .

Gragg, J., Cloutier, A., & Yang, J. (2013). Optimization-based posture reconstruction for digital human models. *Computers & Industrial Engineering*, *66*(1), 125–132.

Gürdür Broo, D., Kaynak, O., & Sait, S. M. (2022). Rethinking engineering education at the age of industry 5.0. *Journal of Industrial Information Integration*, *25*, 100311.

Hignett, S., & McAtamney, L. (2000). Rapid entire body assessment (REBA). *Applied Ergonomics*, *31*(2), 201–205.

Joshi, M., & Deshpande, V. (2019). A systematic review of comparative studies on ergonomic assessment techniques. *International Journal of Industrial Ergonomics*, *74*, 102865.

Korhan, O. (2019). Work-related musculoskeletal disorders. Rijeka: IntechOpen. https://doi.org/10.5772/intechopen.78458

Liu, X., Lv, J., Xie, Q., Huang, H., & Wang, W. (2020). Construction and application of an ergonomic simulation optimization method driven by a posture load regulatory network. *Simulation*, *96*(7), 623–637.

Longo, F., Padovano, A., & Umbrello, S. (2020). Value-oriented and ethical technology engineering in industry 5.0: A human-centric perspective for the design of the factory of the future. *Applied Sciences*, *10*(12).

Lu, Y., Zheng, H., Chand, S., Xia, W., Liu, Z., Xu, X., Wang, L., Qin, Z., & Bao, J. (2022). Outlook on human-centric manufacturing towards industry 5.0. *Journal of Manufacturing Systems*, *62*, 612–627.

Ma, L., Zhang, W., Chablat, D., Bennis, F., & Guillaume, F. (2009). Multi-objective optimisation method for posture prediction and analysis with consideration of fatigue effect and its application case. *Computers & Industrial Engineering*, *57*(4), 1235–1246.

Maddikunta, P. K. R., Pham, Q.-V., Prabadevi, B., Deepa, N., Dev, K., Gadekallu, T. R., Ruby, R., & Liyanage, M. (2022). Industry 5.0: A survey on enabling technologies and potential applications. *Journal of Industrial Information Integration*, *26*, 100257.

Marler, R., Arora, J., Yang, J., Kim, H.-J., & Abdel-Malek, K. (2009). Use of multi-objective optimization for digital human posture prediction. *Engineering Optimization*, *41*, 925–943.

Merikh-Nejadasl, A., El Makrini, I., Van De Perre, G., Verstraten, T., & Vanderborght, B. (2021). A generic algorithm for computing optimal ergonomic postures during working in an industrial environment. *International Journal of Industrial Ergonomics*, *84*, 103145.

Mohammadi Zeidi, I., Morshedi, H., & Zeidi, B. (2011). The effect of interventions based on transtheoretical modelling on computer operators' postural habits. *Clinical Chiropractic*, *14*, 17–28.

Mårdberg, P., Fredby, J., Engström, K., Li, Y., Bohlin, R., Berglund, J., Carlson, J. S., & Vallhagen, J. (2018). A novel tool for optimization and verification of layout and human logistics in digital factories. *Procedia CIRP*, *72*, 545–550. 51st CIRP Conference on Manufacturing Systems.

Nakajima, T., Asami, Y., Endo, Y., Tada, M., & Ogihara, N. (2022). Prediction of anatomically and biomechanically feasible precision grip posture of the human hand based on minimization of muscle effort. *Scientific Reports*, *12*.

Nguyen, T. D., Bloch, C., & Krüger, J. (2016). The working posture controller: Automated adaptation of the work piece pose to enable a natural working posture. *Procedia CIRP*, *44*, 14–19. 6th CIRP Conference on Assembly Technologies and Systems (CATS).

Nord Nilsson, L., & Vänje, A. (2018). Occupational safety and health professionals' skills - a call for system understanding? experiences from a co-operative inquiry within the manufacturing sector. *Applied Ergonomics*, *70*, 279–287.

Nourmohammadi, A., Ng, A. H. C., Fathi, M., Vollebregt, J., & Hanson, L. (2023). Multi-objective optimization of mixed-model assembly lines incorporating musculoskeletal risks assessment using digital human modeling. *CIRP Journal of Manufacturing Science and Technology*, *47*, 71–85.

Otto, A., & Battaïa, O. (2017). Reducing physical ergonomic risks at assembly lines by line balancing and job rotation: A survey. *Computers & Industrial Engineering*, *111*, 467–480.

Otto, A., & Scholl, A. (2011). Incorporating ergonomic risks into assembly line balancing. *European Journal of Operational Research*, *212*(2), 277–286.

Pistolesi, F., Baldassini, M., & Lazzerini, B. (2024). A human-centric system combining smartwatch and liDAR data to assess the risk of musculoskeletal disorders and improve ergonomics of industry 5.0 manufacturing workers. *Computers in Industry*, *155*, 104042.

Rahman, H. F., Janardhanan, M. N., & Ponnambalam, S. G. (2023). Energy aware semi-automatic assembly line balancing problem considering ergonomic risk and uncertain processing time. *Expert Systems with Applications*, *231*, 120737.

Rodrigues, P. B., Xiao, Y., Fukumura, Y. E., Awada, M., Aryal, A., Becerik-Gerber, B., Lucas, G., & Roll, S. C. (2022). Ergonomic assessment of office worker postures using 3d automated joint angle assessment. *Advanced Engineering Informatics*, *52*, 101596.

Schwarzer, R. (2008). Modeling health behavior change: How to predict and modify the adoption and maintenance of health behaviors. *Applied Psychology*, *57*, 1–29.

Wang, J., Chen, D., Zhang, X., & Zhu, M. (2023). Real-time anthropometric data-driven evaluation method for complex console layout design. *Computers & Industrial Engineering*, *183*, 109463.

Winum, P. C., Ryterband, E. C., & Stephenson, P. (1997). Helping organizations change: A model for guiding consultation. *Consulting Psychology Journal: Practice and Research*, *49*, 6–16.

Wu, T., Zhang, Z., Zhang, Y., & Zeng, Y. (2023). Modelling and optimisation of two-sided disassembly line balancing problem with human-robot interaction constraints. *Expert Systems with Applications*, *230*, 120589.

Xu, S., & Hall, N. G. (2021). Fatigue, personnel scheduling and operations: Review and research opportunities. *European Journal of Operational Research*, *295*(3), 807–822.

Yazdani, A., & Wells, R. (2018). Barriers for implementation of successful change to prevent musculoskeletal disorders and how to systematically address them. *Applied Ergonomics*, *73*, 122–140.

Zhang, M., Shi, R., & Yang, Z. (2020). A critical review of vision-based occupational health and safety monitoring of construction site workers. *Safety Science*, *126*, 104658.

Zhang, Z., Chica, M., Tang, Q., Li, Z., & Zhang, L. (2024). A multi-objective co-evolutionary algorithm for energy and cost-oriented mixed-model assembly line balancing with multi-skilled workers. *Expert Systems with Applications*, *236*, 121221.